Available online at www.sciencedirect.com

ScienceDirect

Procedia Engineering 10 (2011) 3345–3352

Engineering Procedia

ICM11

Fatigue Behavior Of Pipeline Steel Under Hydrogen Environment And Low Temperature

P. Fassina[a], F. Brunella[b], L. Lazzari[b], G. Re[b], L. Vergani[c], A. Sciuccati[c,*]

[a]*Exploration & Production Division, ENI, Via Emilia 1, 20097 San Donato Milanese, Italy*
[b] *Chemistry, Materials and Chemical Engineering Department "Giulio Natta", Politecnico di Milano, Via Mancinelli 7, 20131 Milano, Italy*
[c]*Department of Mechanical Engineering, Politecnico di Milano, Via La Masa 1, 20156 Milano, Italy*

Abstract

In the presence of H_2S, metallic materials, such as carbon and low alloy steels, may suffer hydrogen damage and hydrogen embrittlement. In this paper the influence of hydrogen and low temperature on mechanical properties of two pipeline materials, X65 micro-alloyed and F22 low alloy steels, is studied. An electrochemical hydrogen charging method has been setup. Diffusible hydrogen content of steels is in the range 0.6 to 2 ppm. Fatigue propagation tests were carried out on charged and uncharged specimens, by varying the test temperature and the frequency of the load application cycle. The experimental results show an evident effect of the hydrogen presence on the fatigue crack growth. The diffusion rate of hydrogen in the steels seems to be the most important parameter in order to explain the influence of temperature and frequency on the fatigue crack propagation rate. Fracture surface examination confirms the results of mechanical testing.

Keywords: Hydrogen embrittlement, Low temperature, Fatigue crack propagation, Pipeline steels

1. Introduction

Carbon steel and low alloy steel are commonly used in Oil and Gas industry when general corrosion due to the presence of CO_2 and H_2S is considered acceptable to stand the design life. However, when sour condition applies, the occurrence of Sulphide Stress Cracking (SSC) in the presence of H_2S on susceptible materials must be investigated [1]. Furthermore, when very low temperatures, e.g., below -40°C, are also present, as in most recent oil&gas fields, a synergistic negative effect may result from the combination of

* Corresponding author. Tel.: +39 339 80 36 978.
E-mail address: augusto.sciuccati@mecc.polimi.it

 doi:10.1016/j.proeng.2011.04.552

sour conditions and low temperatures on the mechanical behaviour of the used materials. To investigate the effect of hydrogen and low temperature on pipeline steels, toughness and crack propagation tests of charged and uncharged specimens were carried out. Toughness tests are described in [2][3]. An electrochemical hydrogen charging method, described in [4], has been setup, avoiding any critical conditions from the point of view of preparation, safety and disposal. The content of hydrogen was controlled and measured in the specimens: the diffusible hydrogen content of steels is always in the range 0.6 to 2 ppm. The effect of hydrogen and low temperature on the fatigue crack propagation is a very important task [5][6][7]: it depends on materials and microstructures.

2. Materials

Experimental activities involved seamless pipes in quenched and tempered conditions manufactured with:

- 2 1/4 Cr 1 Mo steel, ASTM A182 F 22, (outside diameter D=320 mm, wall thickness t=65 mm).
- Micro-alloyed C-Mn steel, API 5L X65, (D=323 mm, t=46 mm);

The F22 [8] pipe is a Q&T pipe from ingot casting-forging-piercing-hot rolling-quench and tempering production route. X65 [9] grade pipe is a Q&T pipe from conventional billet casting-piercing-hot rolling-quench and tempering operations. Both materials are for sour service use, so that they underwent through all the required qualifications. In Table 1 the chemical compositions of the selected materials are reported. X65 steel microstructure is equiaxed and acicular ferrite with finely dispersed carbides. The microstructure is rather homogeneous. Inclusion shape is round. F22 steel microstructure is typical of tempered lath martensite, i.e., elongated ferrite grains with finely dispersed carbides; the microstructure is rather homogeneous; inclusion density is very low; inclusion shape is round. Mechanical properties have been evaluated at room temperature. Results are collected in Table 2.

Table 1. Chemical compositions

Material	C	Mn	Cr	Mo	Ni	Nb	V	Ti
F22	0.14	0.43	2.25	1.04	0.08	0.023	<0.01	<0.01
X65	0.11	1.18	0.17	0.15	0.42	0.023	0.06	<0.01

Table 2. Mechanical properties

Material	σ_{ys} (MPa)	σ_{ts} (MPa)	E (MPa)	A (%)
F22	468±2.7	592±2.1	206500±1500	20±2.5
X65	511±6.7	609±5.7	206208±6049	21±6.5

3. Experimental results

A large number of experimental tests were carried out to characterize the mechanical behaviour and fatigue crack propagation of the uncharged and hydrogen charged steels. C(T) specimens of F22 and X65 steels were manufactured based on ASTM 647 [10], with thickness B=20mm. The specimens were loaded by a 100 kN MTS servo-hydraulic loading frame. All tests were carried out accordingly to ASTM 647 [10]. Tests were carried out in load control, the cyclic load was applied as a sinusoidal wave with ratio R=0.1. Measurement of crack growth was made through the compliance method.

3.1 F22 steel

The uncharged specimens were fatigue tested by varying the test temperature, in particular the following temperatures were considered: Room Temperature (RT), T=-60°C, T=-100°.The effect of temperatures on the uncharged specimens is not significant. Fig. 1 shows the curves da/dN in function of ΔK: these curves are very similar, with the same slope (m≈2.4) and slightly differing in the C values. Propagation tests on uncharged specimens were carried out at a load frequency (f) equal to 20Hz. In these conditions, as widely shown in literature, frequency is not a parameter affecting growth rate. It should be pointed out that variations between crack growth rate at different temperatures are very small and that crack growth rate, at same ΔK, decrease while decreasing temperature, as expected. Indeed, cyclic plastic zone is reduced while decreasing temperature because yield strength is increased, at the same time.

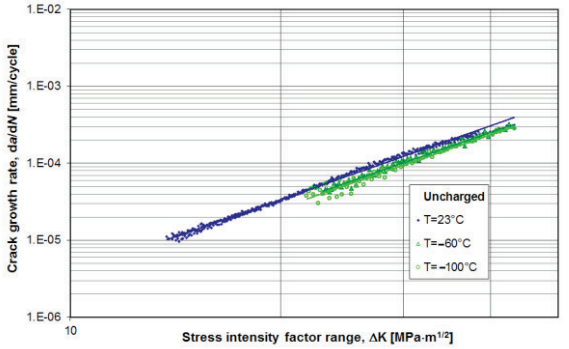

Fig. 1. F22 steel: crack growth rate for uncharged specimens at different temperatures

Fig. 2 shows the fatigue crack propagation results for the hydrogen charged specimens, at room temperature by varying the frequency. In particular the considered frequencies are: f=1Hz and f=10Hz. In the same Figure the uncharged crack propagation results (blue line) are compared. Fig. 3 shows the results for specimens tested at T=-30°C and f=1 Hz and f=10 Hz.

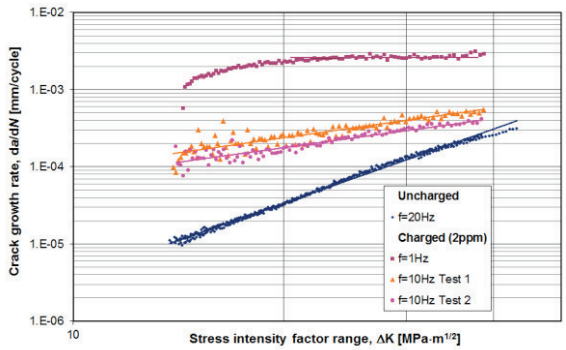

Fig. 2. F22 steel: crack propagation rates, by varying the frequency at room temperature

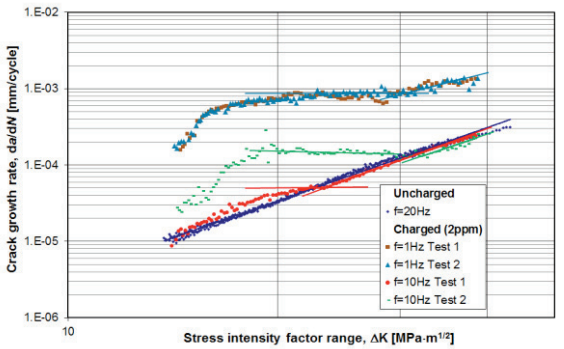

Fig. 3. F22 steel: crack propagation rates, by varying the frequency at T=-30°C

3.2 X65 steel

Fig. 4 shows the crack propagation rate curve obtained by the uncharged specimens at room temperature. The curve is interpolated by two lines with different slopes: $m\approx4$ in the first part, at low ΔK value, and $m\approx2.4$ in the second part, at larger ΔK values. In the same Figure the curves by the hydrogenated specimens, at room temperature and frequency: f=1Hz and f=10 Hz, are shown. Fig.5 shows the crack growth rate by the hydrogenated specimens at T=-30°C and f=1 Hz and f=10 Hz.

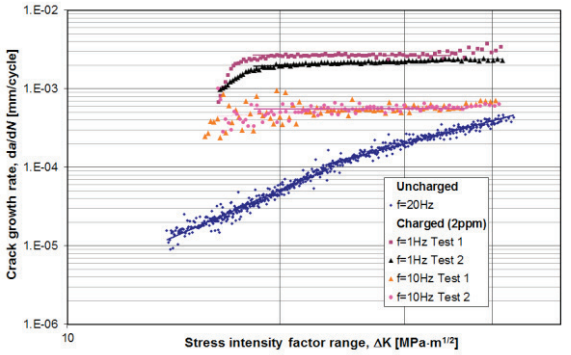

Fig. 4. X65 steel: crack propagation rates, by varying the frequency at room temperature

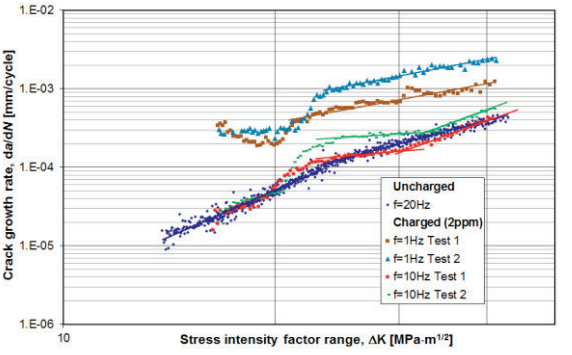

Fig. 5. X65 steel: crack propagation rates, by varying the frequency at T=-30°C

4. Discussion

The effect of hydrogen is evident both in F22 and X65 specimens. The hydrogen charge causes, in fact, embrittlement and crack growth acceleration in all the considered conditions.

4.1 F22 steel

The effect of hydrogen is particularly evident when f=1Hz: in this case "plateau" regions are easily noticeable (see Fig.2). Starting from a threshold value is $\Delta K_{th}\approx15\div17 MPa\sqrt{m}$ crack growth rate increases with respect to the value of uncharged specimens and reaches a constant value ($da/dN\approx2\div3\cdot10^{-3}$mm/cycle) independent from crack length and load level. The presence of "plateau" regions is a typical feature of the interaction between corrosion fatigue and stress corrosion cracking phenomena, that can result in mechanisms called: true corrosion fatigue, stress corrosion fatigue and combination of the previous [11][12].

When f=10Hz the effect of hydrogen is evident, but lower with respect of the case with f=1Hz. The effect depends also on the ΔK values: at low ΔK (till $\Delta K\approx35 MPa\sqrt{m}$), in fact, embrittlement due to hydrogen is clearly significant, but at higher values of ΔK, crack propagation rate becomes similar to the uncharged specimen one. This phenomenon can be interpreted as it follows: crack growth rate is the result of a combination of two phenomena, namely: the mechanical damage (frequency dependent) and the hydrogen one (time dependent), at low ΔK in a range of about $15\div35$ $MPa\sqrt{m}$ hydrogen effect is predominant, while for higher values of ΔK mechanical effect, due to high loads, becomes predominant. In the last case, the fatigue behavior is mainly controlled by the mechanical properties of the material (as

if it were hydrogen free) since there is not enough time for hydrogen to reach the crack tip because of the high crack growth rate. Again by observing Fig. 2, the curve of hydrogen charged specimen at f=1Hz and room temperature shows a strong enhancement of the embrittlement effect because of the long load application times and temperature that facilitate hydrogen diffusion at crack tip. Fig. 3 shows the results at T=-30°C and frequencies f=1 and f=10 Hz. Also in this condition, a plateau region is observed for the charged specimens; however it was noted a smaller embrittlement effect of the hydrogen. Especially at high ΔK values and f=10Hz, the crack growth rate of the charged specimens is similar to one of the uncharged specimens.

4.2 X65 steel

Fig. 4 shows an evident "plateau" trend of the charged specimens both if f=1Hz ($da/dN \approx 2 \div 3 \cdot 10^{-3}$ mm/cyc) and f=10Hz ($da/dN \approx 5 \div 7 \cdot 10^{-4}$mm/cyc) and room temperature. The threshold value is $\Delta K_{th} \approx 15 \div 17 MPa\sqrt{m}$. Fig. 5 shows the crack growth rate, when T=-30°C. Also at this test temperature, the crack growth rate of the charged specimens is largely independent on ΔK; however the embrittlement effect of the hydrogen is lower. Especially at high ΔK values and f=10 Hz, the crack growth rate of the charged specimens approaches the behavior of the uncharged specimens.

5 Fracture surface examination

The fracture surface have been examined for both materials and different experimental conditions. In the following, only the results for X65 steel will be presented.

In Fig. 6 the macroscopic image of the fracture surface for X65 specimens is shown. The specimen without hydrogen tested at room temperature displays the typical flat, featureless appearance up to the final mechanical failure when a critical J value is reached, so that it is difficult to distinguish between the fatigue pre-crack and the further crack extension during the fatigue test, see fig. 6(a).

Hydrogenated specimens tested at room temperature at 10 Hz , fig. 6(b) and 1 Hz, fig. 6 (c) still display a rather flat semi-elliptical fatigue surface in the specimen centre, with a coarser fracture at the border before final mechanical failure.

Hydrogenated specimens tested at -30 °C and 10 Hz or 1 Hz, figure 6 (d), (e) show two very different crack growth stages and the separation point roughly corresponds to the crack depth where the slope of the da/dN vs. ΔK curves suddenly increases (Fig. 5). In the first stage fatigue fracture surface is rather flat with small feather-like features, while in the second stage fracture is much more fragmented, surface is rough, feather-like features are much bigger and crack appears branched as it is demonstrated by detached fragments of steel on the fracture surface in particular fig. 6 (e) in the centre.

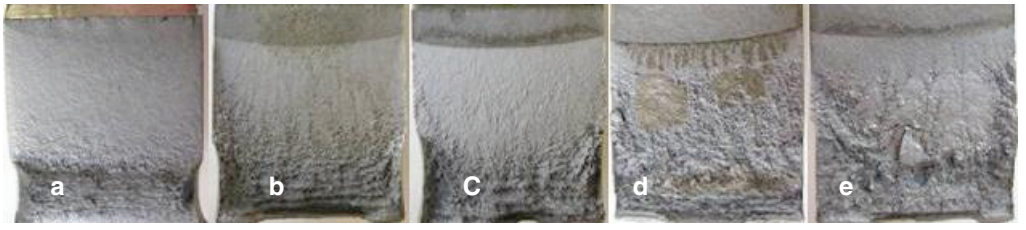

Figure 6 Macroscopic appearance of the fracture surface, X65 specimens (specimen thickness = 20 mm): no hydrogen, R.T. (a); hydrogen charged, R.T. 10 Hz (b), and 1 Hz (c); hydrogen charged, -30°C, 10 Hz (d), and 1 Hz (e)

The fracture surface has been analysed by Scanning Electron Microcopy (SEM) along the central axis of the specimen. Fracture surface of the specimen without hydrogen is slightly fragmented (Fig. 7) in the first stage of crack growth (a_0 + 1.5 mm) and it is more flat at the end. Typical fatigue ductile striations are present, but are visible only at high magnification when the crack is short. For long crack (high ΔK values) striations are larger, deeper and visible at low magnification (Fig.8). When the maximum applied K during a cycle reach a critical value, for a crack extension of about 13 mm, the fracture aspect changes to ductile tearing characterized by dimples nucleated by inclusions. The fatigue fracture surface of specimen charged with hydrogen completely changes and depends on test temperature and frequency. At room temperature and a frequency of 10 Hz, moving along the centre of the specimen, at a crack extension equal to a_0 + 2 mm, corresponding to the scattered section of the fatigue curve (Fig. 5), fracture is more flat than in the specimen without hydrogen (Fig. 9) and shows small brittle facets (Fig. 10). On these facets some features defined by some Authors as "brittle striations" are present, they are oriented in different directions irradiating from a point and their separation is in the order of $8 \div 9\ 10^{-4}$ mm that is the upper range of values measured during mechanical test.

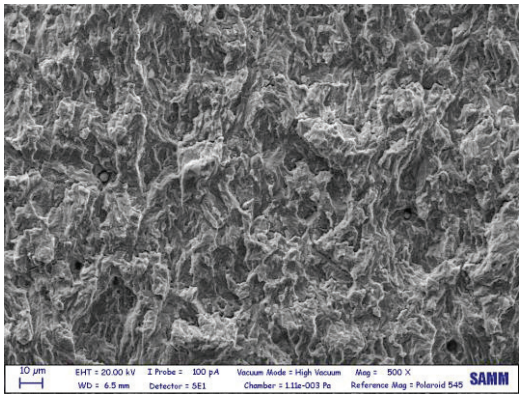

Figure 7 Specimen (no-hydrogen, R.T., 20 Hz) in the mid-thickness at a crack depth of a0 + 1.5 mm, 500x

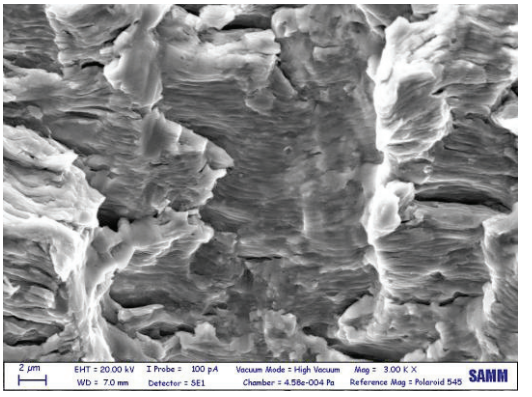

Figure 8 Specimen (no-hydrogen, R.T., 20 Hz) in the mid-thickness at a crack depth of a0 + 11.5 mm, 3000x

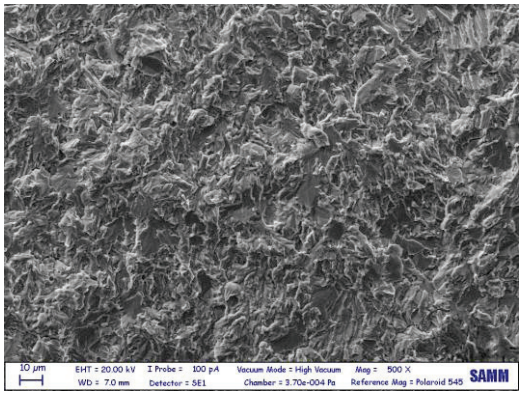

Figure 9 Specimen (hydrogen, R.T., 10 Hz) in the mid-thickness at a crack depth of a0 + 2 mm magnification x500

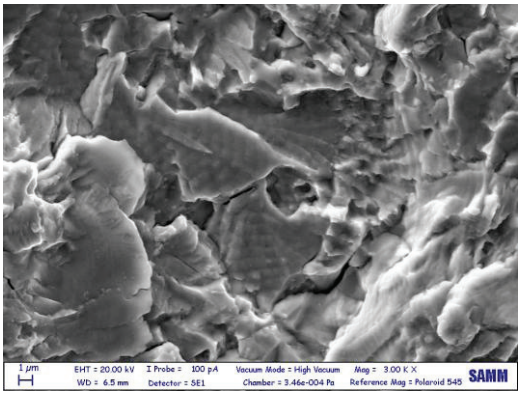

Figure 10 Specimen (hydrogen, R.T., 10 Hz) in the mid-thickness at a crack depth of a0 + 2 mm magnification x3000

Fracture travels on slightly different planes that join together with long, thin, ductile bands parallel to the travelling direction (Fig. 11). These bands can be also seen on the fracture surface at low magnification, see Fig. 6 (b), and are associated to the presence of "cellular" fracture (Fig. 11 a top-centre), already observed on the fracture surface of CT specimens with hydrogen in J-integral tests [3].

At a crack depth of a_0 + 5 mm, where the fatigue curve is almost constant, the fracture surface is still flat with a brittle appearance (Fig. 12) and showing fan-shaped facets larger than the ones observed in the first stage of fatigue propagation. On these fan-shaped facets it is possible to see brittle striations having a distance of about 6÷7 10^{-4} mm, being the mean fatigue crack rate 5.7 10^{-4} mm/cycle. At a crack depth of about a_0 + 7.5 mm fracture becomes partially cellular (Fig. 13), this kind of fracture becomes predominant increasing the crack depth (Fig. 14), the cells become smaller and the percentage of ductile fracture becomes larger. The examination of fracture surface along the crack depth at 5 mm from the right side of the specimen (1/4 of the thickness), gives the same results, the only difference is that cellular fracture initiates for a shorter crack propagation approaching to the specimen side and this produces the semi-elliptical shape that can be seen in the picture of Fig. 6 (b).

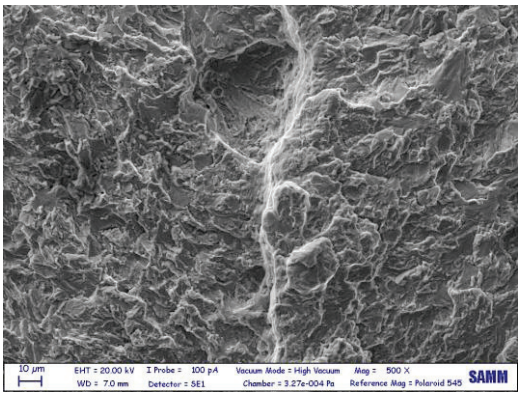

Figure 11 Specimen (hydrogen, R.T., 10 Hz) in the mid-thickness at a crack depth of a0 + 2 mm magnification x500

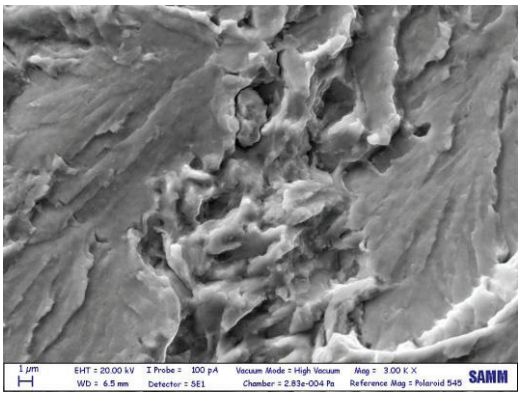

Figure 12 Specimen (hydrogen, R.T., 10 Hz) in the mid-thickness at a crack depth of a0 + 5 mm magnification x3000

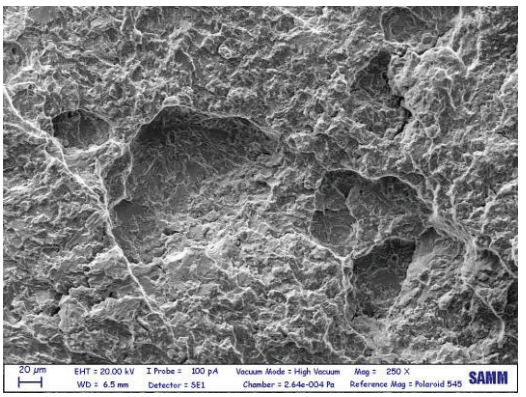

Figure 13 Specimen (hydrogen, R.T., 10 Hz) in the mid-thickness at a crack depth of a_0 + 7.5 mm magnification x250

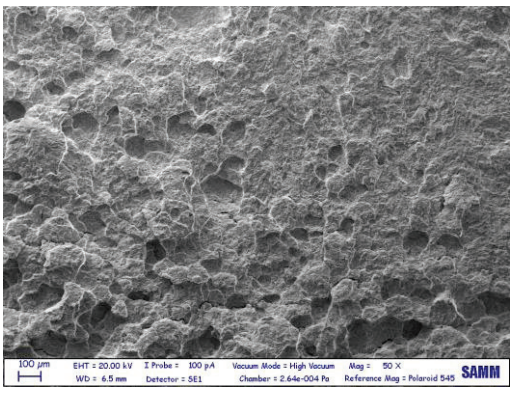

Figure 14 Specimen (hydrogen, R.T., 10 Hz) in the mid-thickness at a crack depth of a_0 + 9.5 mm magnification x50

6 Conclusions

The influence of hydrogen on the fatigue properties of two steels was investigated by fatigue crack propagation tests. Hydrogen effect was clearly observed and influenced by load frequency and temperature: low frequencies allow the hydrogen to migrate at the crack tip, as a consequence hydrogen embrittlement effect on crack growth rate are enhanced; low temperature reduce the mobility of hydrogen in the lattice (i.e. reduce diffusion coefficient), reducing the embrittlement effect.

Crack growth rate is the sum of two contributions: one named "mechanical" that depends on applied loads and a second due to hydrogen effect. When crack growth rate increases, the "mechanical" contribution prevails because hydrogen atoms do not have enough time to accumulate at the crack tip: as a consequence crack growth rate is no longer hydrogen dependent.

Fractographic examinations demonstrate that for higher temperature and lower frequency, when crack growth rate is higher, brittle fracture mechanisms are present.

Acknowledgements

The authors would like to thank ENI-Exploration & Production Division, for having supported the research and for their permission to publish this paper, Tenaris and Ringmill for the supplied material, Centro Sviluppo Materiali S.p.A. for the cooperation in experimental tests (hydrogen measurements).

References

[1] EFC Publication nr. 16. Guidelines on Materials Requirements for Carbon and Low Alloy Steels for H_2S-Containing Environments in Oil and Gas Production. Cambridge: The Institute of Materials; 2002.

[2] Fassina P, Morana R, Alleva L, Mortali G, Vergani L, Sciuccati A. Materials behavior in extreme conditions: influence of large amounts of H_2S on steel toughness in low temperature environments. *Proceedings of European Corrosion Congress EUROCORR;* 2010 Sep 13-17; Moscow; 2010.

[3] Fassina P, Bolzoni F, Fumagalli G, Lazzari L, Vergani L, Sciuccati A. Influence of hydrogen and low temperature on pipeline steels mechanical behaviour. *Proceedings of International Conference on the mechanical behavior ICM11;* 2011 Jun 5-9; Como (Italy); 2011.

[4] Bolzoni F., Fassina P., Fumagalli G, Lazzari L, Re G. Hydrogen charging of carbon and low alloy steel by electrochemical methods. *Proceedings of European Corrosion Congress EUROCORR*; 2010 Sep 13-17; Moscow; 2010.

[5] Murakami Y, Matsuoka S. Effect of hydrogen on fatigue crack growth of metals. *Engineering Fracture Mechanics* 2010;77:1926-1940.

[6] Kanezaki T, Narazaki C, Mine Y, Matsuoka S, Murakami Y. Effects of hydrogen on fatigue crack growth behavior of austenitic stainless steels. *International Journal of Hydrogen Energy* 2008;33:2604-2619.

[7] Murakami Y. Metal Fatigue: Effects of Small Defects and Nonmetallic Inclusions. Oxford: Elsevier; 2002.

[8] ASME BPVC Section II SA-182, Specification for forged or rolled alloy-steel, pipe flanges, forged fittings and valves and parts for high-temperature service. New York: The American Society of Mechanical Engineers; 2004.

[9] API Specification 5L, Specification for Line Pipe. Washington: American Petroleum Institute; 2004.

[10] E 647-08, Standard Test Method for Measurement of Fatigue Crack Growth Rates. Annual book of ASTM standards 2008. West Conshohocken, USA: American Society of Testing and Materials; 2008.

[11] McEvily AJ, Wei RP. In Corrosion Fatigue: chemistry, mechanics and microstructure. Devereux O., McEvily AJ, Staehle RW (eds.). Houston: National Association of Corrosion Engineers; 1972: 381-395.

[12] Sinigaglia D, Re G, Pedeferri P. Cedimento per fatica e ambientale dei materiali metallici. Milano: CLUP; 1979.